Journal of Magnetism and Magnetic Materials 401 (2016) 44–49

Contents lists available at ScienceDirect

Journal of Magnetism and Magnetic Materials

journal homepage: www.elsevier.com/locate/jmmm

Structure and magnetic transport properties of $GdIn_{3-x}Mn_x$ intermetallics

Qiang He, Yongquan Guo *, Hanyuan Liu

North China Electric Power University, School of Energy Power and Mechanical Engineering, Beijing 102206, China

ARTICLE INFO

Article history:
Received 4 August 2015
Received in revised form
25 September 2015
Accepted 4 October 2015
Available online 9 October 2015

PACS:
61.05.cp
75.50.Ee
75.30.Cr
75.47.-m

Keywords:
$GdIn_{3-x}Mn_x$
Antiferromagnetic order
Magnetic transport

ABSTRACT

The crystal structures and magneto-transport properties of $GdIn_{3-x}Mn_x$ have been investigated using X-ray diffraction and magnetic and electric measurements. $GdIn_{3-x}Mn_x$ crystallize in cubic structure, and their lattice parameters tend to decrease with increasing Mn content due to the size effect at In site by Mn substitution for In. Mn doped $GdIn_{3-x}Mn_x$ order antiferromagnetically at low temperature. However, Mn doping into $GdIn_3$ causes the decrease of Néel temperature due to the distortion of $Gd(In,Mn)_3$ tetrahedron formed by Gd at corners and (In,Mn) at face centers in unit cell. The resistivities of $GdIn_{3-x}Mn_x$ are going up with increasing Mn content. The electric phase transition is associated with the magnetic transition, and the magneto-transport follows electron–magnon scattering model in low temperature region and the Stoner spin fluctuation model in high temperature region, respectively.

1. Introduction

Most of RX_3 intermetallic compounds (R=rare earth; X=In, Ga, Tl, Sn and Pb) have cubic $AuCu_3$-type crystal structure [1,2]. The interest is growth on RX_3 due to their salient features such as formation of magnetic moment, crystal field effect and multiaxial magnetic structures [3–5]. More recently, the new physical phenomena such as heavy Fermion and superconductor in critical conditions (super low temperature or super high pressure) have been observed in RIn_3 [6,7]. The antiferromagnetism has been observed in most of RIn_3 intermetallics [8]. However, the highest Néel temperature is only 48 K for $GdIn_3$. It originates from the 4f electronic configures of Gd ion. The orbit momentum of Gd ion is frozen ($L=0$) due to its half-filled 4f shell, and the magnetic moment only depends upon the spins of unpaired 4f electrons. The effective magnetic moment equals to 8.20 μ_B, it is closed to that of Gd ion. It implies that the contribution to the effective magnetic moment originates from Gd ion. The paramagnetic Curie–Weiss temperature is −85 K [9]. The electric transport properties of $GdIn_3$ in the paramagnetic range are similar to those of the other RIn_3 intermetallic compounds, and its Fermi surface is almost the same as that of non-magnetic intermetallic compound $LaIn_3$ [10].

Previous studies have been mainly focused on the doping effects on structure and magnetic properties at In site or R site by substituting the semiconductor element Sn for In [11,12] or the other rare-earth element for Gd [13]. It is well known that the 3d transition metal Mn has played important roles in magnetic materials due to its significant contributions to the magnetic anisotropy by coupling with 4f electrons of the rare-earths [14–16]. The ternary intermetallic compound $Gd(Mn_{1-x}In_x)_2$ exhibits interesting physical properties. The temperature of its spontaneous magnetization is 220 K lower than the ordering temperature T_C, while the ferromagnetic order occurs at 120 K [14]. A spin glass-like phenomenon in figuration of the Mn moment has been observed in GdMnIn intermetallic compound [15,16]. In this study, we design the ternary alloys with a formula of $GdIn_{3-x}Mn_x$ by doping small amount of Mn into $GdIn_3$. It is expected to improve the magnetic properties and electric transport by 3d–4f coupling interactions between Mn and Gd.

2. Experimental details

$GdIn_{3-x}Mn_x$ ($x=0.0$, 0.1, 0.2, 0.3) were prepared using arc melting with 10 wt% excess of Mn to compensate for the weight loss during the melting under a protective ultra-pure argon gas. The purities of starting materials were more than 99.9%. To ensure the homogeneity of ingots, the samples were turned upside down

* Corresponding author. Fax: +86 10 61772383.
E-mail address: yqguo@ncepu.edu.cn (Y. Guo).

http://dx.doi.org/10.1016/j.jmmm.2015.10.004
0304-8853/

and re-melted for 4 times. The ingots were wrapped with Ta foil and annealed at 800 °C for 5 days in an evacuated quartz tubes, and followed by quenching in water.

The phases in $GdIn_{3-x}Mn_x$ were checked by using a Rigaku automatic X-ray diffractometer with Cu-$K_{\alpha 1}$-radiation. After normalization, the diffraction peaks were indexed for determining the planar induces and lattice parameters. The X-ray diffraction data were analyzed using the Rietveld powder diffraction profile-fitting technique for determining crystal structure of $GdIn_{3-x}Mn_x$. According to the refined structure parameters, the distortions of $R(In,Mn)_3$ tetrahedron and $(In,Mn)_6$ octahedron formed by Gd at corners and (In,Mn) at face centers have been investigated with Diamond program. The bond lengths of Gd–(In,Mn) and (In,Mn)–(In,Mn) and bond angles of (In,Mn)–Gd–(In,Mn) are estimated based on the atomic ordinates of Gd and (In,Mn) in unit cell.

The temperature dependence of magnetization for $GdIn_{3-x}Mn_x$ was measured using a SQUID magnetometer (MPMS XL7 Quantum Design) in temperature ranging from 2 to 300 K with applying a magnetic field of 1 kOe. The magnetizing curves of $GdIn_{3-x}Mn_x$ were measured with applying the fields from 0 to 50 kOe at 2 K. The temperature dependence of resistivity $\rho(T)$ was measured by means of a standard four-probe technique in temperature ranging from 5 K to 300 K without applying any external field.

3. Results and discussion

3.1. Crystal structure

The $GdIn_{3-x}Mn_x$ samples show the single phase based on the analysis of powder X-ray diffraction (XRD) patterns, as shown in Fig. 1. The X-ray diffraction peaks of $GdIn_{3-x}Mn_x$ could be indexed as a primary cubic structure. The atomic occupations have been determined with Rietveld method. For the structural refinement, the Voigt function has been adopted as a structural model to simulate the diffraction peak shapes of $GdIn_{3-x}Mn_x$. The typical refined XRD patterns for the sample with $x=0.3$ is shown in Fig. 2, where the measured and calculated XRD patterns are marked with the symbol of "+" and solid line, respectively. The lowest trace indicates the differences between the two patterns. Based on the structural refinement, $GdIn_{3-x}Mn_x$ crystallizes a cubic $AuCu_3$-type structure with a space group of $Pm\bar{3}m$. The atomic occupations correspond to the 1a (0, 0, 0) site for Gd atoms, and the 3c (0.5, 0.5,

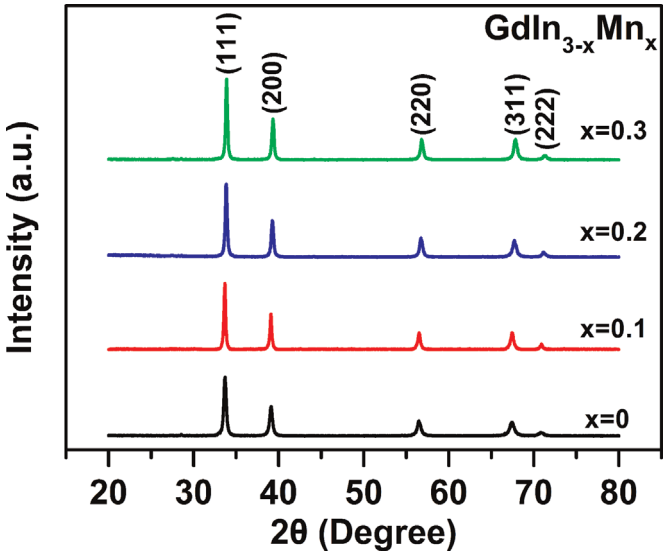

Fig. 1. X-ray diffraction patterns of $GdIn_{3-x}Mn_x$.

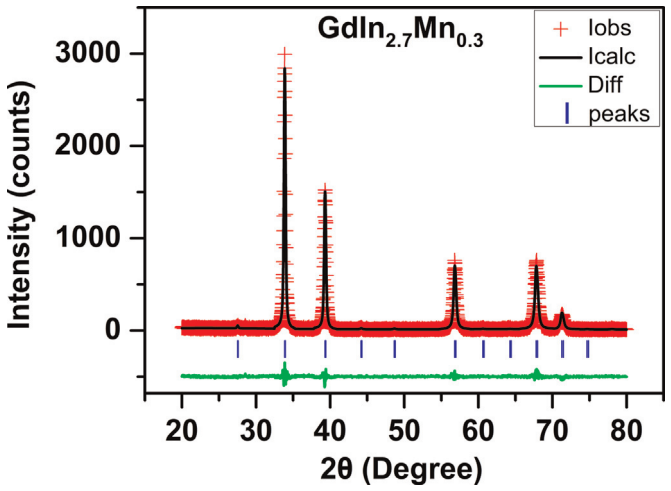

Fig. 2. The refined X-ray diffraction patterns of $GdIn_{2.7}Mn_{0.3}$.

Table 1
The refined structure parameters of $GdIn_{3-x}Mn_x$.

Sample		$GdIn_3$	$GdIn_{2.9}Mn_{0.1}$	$GdIn_{2.8}Mn_{0.2}$	$GdIn_{2.7}Mn_{0.3}$
Space group		$Pm\bar{3}m$	$Pm\bar{3}m$	$Pm\bar{3}m$	$Pm\bar{3}m$
Z		1	1	1	1
a (Å)		4.605 (5)	4.597 (0)	4.589 (3)	4.580 (0)
Gd 1a (0,0,0)	x	0	0	0	0
number	y	0	0	0	0
	z	0	0	0	0
	N	1	1	1	1
In 3c (1/2,1/2,0)	x	1/2	1/2	1/2	1/2
number	y	1/2	1/2	1/2	1/2
	z	0	0	0	0
	N	3	2.89	2.80	2.69
Mn 3c(1/2,1/2,0)	x	–	1/2	1/2	1/2
number	y	–	1/2	1/2	1/2
	z	–	0	0	0
	N	–	0.11	0.20	0.31
R_p (%)		10.57	9.87	10.34	9.68
R_{wp} (%)		14.67	13.82	14.19	13.45
s		1.39	1.42	1.37	1.41

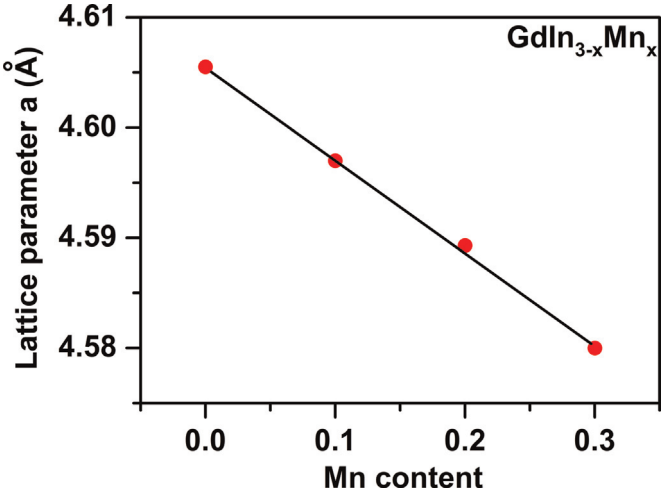

Fig. 3. Mn content dependence of lattice parameters for $GdIn_{3-x}Mn_x$.